Shape and core-excited resonances in electron scattering from alanine

Alexandra Loupas[1, a)] and Jimena D. Gorfinkiel[2, b)]

[1)] *Laboratório de Colisões Atómicas e Moleculares, CEFITEC, Departamento de Física, Faculdade de Ciências e Tecnologia, Universidade Nova de Lisboa, Campus de Caparica, 2829-516, Portugal*

[2)] *School of Physical Sciences, The Open University, Walton Hall, Milton Keynes, MK7 6AA, United Kingdom.*

(Dated: 10 January 2019)

We present detailed *ab initio* scattering calculations using the R-matrix method for electron collisions with the most stable conformer of α-alanine. The shape resonances we identify are in good agreement with earlier calculations and experiments. Core-excited and mixed-character resonances are identified and characterized computationally for the first time. Dissociative electron attachment results are discussed in relation to the resonances identified.

PACS numbers: 34.80-i,34.80.Bm,34.80.Gs

Keywords: electron scattering, resonances

[a)] School of Physical Sciences, The Open University, Walton Hall, Milton Keynes, MK7 6AA, United Kingdom

[b)] Electronic mail: Jimena.Gorfinkiel@open.ac.uk

I. INTRODUCTION

Understanding and modelling the effect of ionizing radiation on biological matter requires, among other data, information on how low energy electrons interact with the molecules in the medium[1]. One of the most relevant electron-induced processes is dissociative electron attachment (DEA), that leads to the break-up of the target via the formation of a temporary negative ion or resonance. For this reason, both DEA and resonance formation in biological molecules has received significant attention over the last couple of decades[2]. Both experimental and theoretical work has focused mainly on DNA constituents, as DNA is the most radiation-sensitive component of a cell. However, other cell constituent are also affected by radiation and their damage could have biological effects. Proteins are one such molecule; similarly to the case of DNA, experiments and calculations have focused on the building blocks of proteins, aminoacids, as these are easier to investigate. Glycine, the simplest aminoacid, has been the most widely studied[1] but results are also available for several others, among them alanine. All the investigated aminoacids show the presence of a low-lying π^* shape resonance associated to the double C=O bond of the carboxyl group.

Aflatooni *et al.*[3] used electron transmission spectroscopy (ETS) to determine vertical attachment energies for the lowest-lying temporary anion state of five aminoacids in the gas phase: glycine, alanine, phenylalanine, tryptophan, and proline. In alanine, they found the π^* resonance around 1.8 eV.

Several theoretical methods have been applied to the study of shape resonances in alanine. Panosetti *et al.*[4] performed calculations that investigated resonance formation and fragmentation for the four smallest aminoacids. A resonance centred at approximately 3 eV was detected for all of them, corresponding again to the π^* resonance. Several higher energy (above 9 eV) shape resonances were also identified and discussed by these authors.

Fujimoto *et al.*[5,6] used the R-matrix method to investigate shape resonance formation for the nine lowest-energy conformers of α-alanine. Two resonances were identified for all conformers: the π^* resonance already mentioned, found in the energy range 2.5-3.2 eV and another shape resonance located in the energy range 9.0-9.8 eV. A third resonance, lying energetically between these two, was identified for the conformers with the largest dipole moment, but not discussed. More recently, Nunes *et al.*[7] used the SMC method to study both positron and electron elastic scattering from alanine. They also identified two resonances

for the lowest energy conformer, with positions in excellent agreement with Fujimoto *et al.*.

DEA experiments were carried out for alanine by Ptasińska *et al.*[8], Vasil'ev *et al.*[9] and Scheer *et al.*[10]. Ptasińska *et al.* measured yields for 9 different anions, with the dehydrogenated parent anion being the most abundant at low energies. They ascribed the peaks in the anion yields above 5 eV to core-excited resonances. Scheer *et al.* and Vasil'ev *et al.* observed similar fragmentation patterns to Ptasińska *et al.*. Abouaf[11] measured the formation of the dehydrogenated parent ion and found a peak at around 1.2-1.3 eV in agreement with all other DEA experiments.

Finally, we mention for completeness that cross section measurements were performed by Marinković *et al.*[12], in the energy range of 40-80 eV and scattering angles from 10 to 150^o. These authors measured directly the DCS using a crossed beam system, and derived the absolute cross sections by normalizing to theoretical results, obtained with the Screen Corrected Additivity Rule procedure, up to 10000 eV. Fujimoto *et al.* determined integral and differential elastic cross sections below 10 eV for several conformers as well as averaged cross sections taking into account relative populations of different conformers[6].

In this paper, we present high-level R-matrix calculations carried out to investigate the resonant spectrum of α-alanine in its most stable conformer I. Both shape and core-excited resonances have been investigated in detail (the low energy resonances are also investigated for two other conformers). The results for the shape resonances agree reasonably well with earlier calculations. We discuss the link of the resonances identified and the results of DEA experiments.

II. THE R-MATRIX METHOD

The R-matrix method has been extensively applied to the study of electron-molecule collisions at low energies. Since the details of the method have been described elsewhere[13], here we summarise its basic underpinning ideas and how it is applied. Our calculations have been performed within the fixed-nuclei approximation; in other words, we have neglected nuclear motion and kept nuclei fixed in the ground state equilibrium geometry of the target molecule. We have used the UKRmol+ suite[14,15], a completely re-engineered version of the UKRmol suite[16] that enables, among other things, the use of larger R-matrix radii.

The R-matrix method is based on the division of space into and inner and outer region,

separated by a sphere of radius a. In the inner region, the scattering electron is indistinguishable from the target electrons and therefore exchange and correlation effects must be taken into account. In the outer region, the scattering electron becomes distinguishable and exchange between it and electrons of the target molecule can be neglected. In order for the method to be valid, the R-matrix radius a must be such that the charge densities of all target electronic states of interest (as well as the (N+1)-electron configurations χ_i, see below) are negligible in the outer region.

In the inner region, the set of basis functions Ψ_k that describe the target plus scattering electron, i.e. the (N+1)-electron system, are expanded as follows:

$$\Psi_k^{N+1} = \mathcal{A} \sum_{i=1}^{n} \sum_{j=1}^{n_c} \Phi_i(\mathbf{x}_N; \hat{r}_{N+1}; \sigma_{N+1}) \frac{u_{ij}(r_{N+1})}{r_{N+1}} a_{ijk} + \sum_{i=1}^{m} \chi_i(\mathbf{x}_{N+1}) b_{ik} \quad (1)$$

where $\mathbf{x}_N$ and $\mathbf{x}_{N+1}$ stand for the space and spin coordinates of all N/N+1 electrons, respectively. σ_{N+1}, r_{N+1} and $\hat{\mathrm{r}}_{N+1}$ stand for the spin, radial and angular coordinates of the scattering electron. The wave function Φ_i describes the ith electronic state of the (N-electron) target together with the angular and spin behaviour of the scattering electron. The functions $\frac{u_{ij}(r_{N+1})}{r_{N+1}}$ describe the radial part of the wave function of the scattering electron. The L^2-integrable functions χ_i, built from target orbitals, describe the short-range polarisation-correlation effects and are crucial for an accurate description of resonances. Finally, $\mathcal{A}$ is the antisymmetrization operator, and the coefficients a_{ijk} and b_{ik} are determined by the requirement that the functions Ψ_k^{N+1} diagonalise the non-relativistic Hermitian (N+1)-Hamiltonian in the inner region.[13]

In the outer region, the interaction potential between the scattering electron and the target molecule is approximated by a single-centre multiple expansion potential. The basis functions Ψ_k^{N+1} are used to construct the R-matrix at the boundary between the regions. This R-matrix is propagated to an asymptotic region where, by matching with known asymptotic expressions, the K-matrix is determined. All relevant scattering quantities can be extracted from the K-matrix or the T- and S-matrices obtained from it.

Scattering calculations can be performed at different levels of approximation; each level corresponds to a certain choice of target electronic states and L^2 functions to be included in

expansion (1). At Static-Exchange (SE) level, only the target ground state wavefunction is included in the expansion and the only L^2 configurations used correspond to the scattering electron occupying a few target virtual orbitals (orbitals unoccupied in the ground state configuration of the target molecule). The SE level only describes shape resonances poorly.

At the Static-Exchange plus Polarization (SEP) level the molecule is allowed to be polarized by the incoming electron; this effect is described by adding to the L^2 configurations used in the SE model, some in which two electrons (scattering and target) can occupy a set of virtual orbitals (VOs). These new L^2 configurations correspond to single excitations from the ground state configuration of the target molecule (normally the core orbitals are kept frozen, i.e. excitations from these orbitals are not allowed). Again, only the target ground state wavefunction is included in expansion (1). The SEP model describe shape resonances very well and some core-excited resonances poorly. In the SE and SEP approximations, the target molecule is described at the Hartree-Fock (HF) level.

In the more sophisticated close-coupling (CC) model, a number of target electronic excited states are included in expansion (1). A complete active space (CAS) approach is used to describe these states. Two types of L^2 configurations are used: (i) those in which the scattering electron is allowed to occupy one of the orbitals in the active space; (ii) those in which the scattering electron is allowed to occupy a set of VOs.[17]

In scattering calculations, one should ensure balance: the description of the N-electron target states Φ_i and the(N+1)-electron basis functions Ψ_k^{N+1} should be of the same quality. In practice, this means that the number of VOs used for the χ_i should be chosen carefully, to avoid either under or overcorrelating the wavefunctions.

In order to identify and characterise the resonances of alanine we analysed the eigenphase sum, and the time-delay[18]. A resonance appears in the eigenphase sum as a jump of approximately π radians[19] that can be fitted with the Breit-Wigner formula. In the case of the time-delay, resonances appear as Lorentzian peaks in the largest eigenvalues of the Q-matrix[20] that can also be fitted with a relatively simple formula. Therefore, the position and width of resonances can be determined from these fits.

III. CHARACTERISTICS OF THE CALCULATION

Alanine, see chemical structure of conformer I in Figure 1, is a molecule with no symmetry that belongs to the C_1 point group; it has 48 electrons. Its vertical ionization threshold is[21] 8.88 eV, its first electronic excitation threshold is[11] 5.4 eV and its spherical polarizability is[22] around 45 a_0^3. The measured dipole moment of alanine is[23] 1.8 Debye but accurate calculations give the value[23,24] of 1.4 Debye.

There are several low-lying structural conformers of this molecule[23–25] whose energy is very close; for this reason, several of these can coexist in the gas used for experiments. Through the potential energy surface analysis for neutral α-alanine, Császár[24] found 13 conformers, and determined several of their properties: conformer I, identified as the most stable, has been our choice for this study. Császár's calculations are in good agreement with the more recent work by Jarger *et al.*[26].

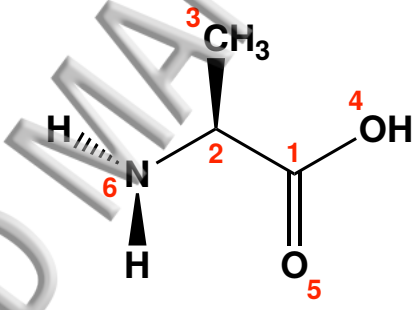

FIG. 1. Schematic chemical structure of conformer I of α-alanine.

The electronic excited states of alanine were studied by Osted *et al.*[27] using a coupled-cluster approach: they identified nine electronic excited states (singlets and triplets) within the 5.9-8.3 eV energy range. Kumar *et al.*[28] studied the infrared, Raman and electronic spectra of alanine, comparing their measurements with *ab initio* calculations (using AM1, RHF and DFT and several basis sets) and identified four singlet states within the energy range of 6.6-9.8 eV. Their calculations are in reasonable agreement with Osted's. Finally, Abouaf[11] investigated the excitation of electronic states below 10 eV and resonant vibrational excitation around 2 eV using ETS: five electronic states were found found between 5 and 10 eV; again, their energies are in reasonable agreement with previous calculations.

A. Target model

In our calculations, we have used the ground state equilibrium geometry of conformer I determined by Császár[24] at the MP2 level of theory. HF and state-averaged CASSCF calculations (SA-CASSCF) have been performed and a number of basis sets tested: 6-31G*, 6-311G**, 6-311++G** and cc-pVDZ. Several active spaces, (8,6), (10,6) and (8,8) and state-averaging schemes (including the 2, 3 and 4 lowest energy states) were also tested, to find the best model for the description of the ground and excited states of alanine. These calculations were performed using the MOLPRO suite[29].

The best results for the excitation thresholds and dipole moment of the ground state were obtained using the (8,6) active space and averaging the 4 lowest states. The excitation thresholds for the lowest 18 states obtained with this CASSCF model and several basis sets are listed in table I. The first three states have very similar thresholds for all basis. As the energy of the states increases, the differences between the results for different basis sets also increase and our description of the excited states gets worse. It is the more diffuse basis set, 6-311++G**, that provides the better agreement with earlier calculations and the experiment. We note that many of the excited states of alanine possesses Rydberg character so it is expected that the more diffuse the basis set will provide a better description. For this basis set, the CASSCF ground state energy is -321.95 Hartree and the dipole moment 1.59 Debye; the HF values are -321.94 Hartree and 1.35 Debye. Accurate calculated values for these quantities are -321.967 Hartree and 1.4 Debye[24].

The somewhat limited models used in R-matrix calculations for the description of the electronic states tend to lead to higher excitation thresholds than those determined experimentally or with more accurate computational methods. In the case of alanine, however, the first five excitation thresholds are smaller (by around 0.5 eV) than those in the literature. This points to a poorer description of the ground state than the excited states.

B. Scattering model

The R-matrix radius was set to a=18 a_0 and GTOs with $l \leq$5 were used to describe the scattering electron. The exponents of the continuum GTOs with $l \leq$4 were optimized by M. Tarana[30] and those for the 7 GTOs with l=5 were optimized by us (the exponents used were

TABLE I. SA-CASSCF vertical excitation energies, in eV, for the electronic excited states of alanine calculated using the active space (8,6) and the following basis set: (A) 6-311G++**, (B) 6-311G** and (C) cc-pVDZ. Also listed are the results of Osted *et al.*[27] calculated using the CCSD/aD(T) model and Kumar *et al.*[28] calculated using the CIS/6-31G model and the experimental data of Abouaf[11]. The label R indicates states of Rydberg character.

	CASSCF			Theory		Exp.
State	A	B	C	Osted	Kumar	Abouaf
1^3A	5.513	5.498	5.517	5.96	-	5.4
1^1A	5.828	5.804	5.828	6.64_R	6.68	6.2
2^3A	6.456	6.665	6.685	7.26_R	-	7.15
3^3A	7.059	6.806	7.092	7.46_R	-	7.85
2^1A	7.197	7.280	7.626	7.55_R	7.97	-
4^3A	8.211	8.369	8.473	7.88_R	-	8.35
3^1A	8.291	8.673	8.783	8.05_R	8.86	-
5^3A	10.256	11.377	11.657	8.3_R	-	-
4^1A	10.445	11.494	11.889	8.79	9.77	-
5^1A	10.771	12.167	12.345	-	-	-
6^3A	12.597	12.484	12.702	-	-	-
7^3A	12.77	12.595	12.9345	-	-	-
6^1A	12.786	12.756	13.052	-	-	-
8^3A	13.023	12.756	13.087	-	-	-
7^1A	13.03	12.875	13.265	-	-	-
8^1A	13.114	12.956	13.479	-	-	-
9^3A	13.295	13.155	13.646	-	-	-
9^1A	13.439	13.229	14.022	-	-	-

0.028469, 0.024413, 0.021097, 0.018250, 0.015743, 0.013491, 0.011406). This value of a is at the limit of when the continuum can be described using GTOs only: the large number of functions needed tends to lead to linear dependence and makes it impossible to orthogonalize bound and continuum orbitals, as required by the implementation of the method. In order to ensure a good enough continuum description, the UKRmol+ suite was used: this suite allows

fog the use of quadruple precision in the calculations thus avoiding linear dependence while allowing significantly smaller deletion thresholds in the orthogonalization step and therefore the use of more continuum functions. These deletion thresholds were set to $1x10^{-17}$ in this work.

The ground electronic state and the lowest 18 excited states, listed in Table I, were included in the CC scattering calculation. These correspond to all states with vertical excitation thresholds up to 13.5 eV.

Unfortunately, it is not possible to determine *a priori* the optimum number of VOs to include in the generation of L^2 configurations[31], i.e. what is the number of VOs to use to avoid both under and overcorrelation. Our approach[17], when experimental data on the shape resonance(s) is available, is to perform the SEP or CC calculation with an increasing number of VOs (selected in energy order) until good agreement with the experimental position of the resonances is achieved. Using this procedure we determined the optimal number of VOs to be 35 for the SEP calculation while all 100 VOs were needed in the CC one.

IV. RESULTS

A. Shape resonances

Figure 2 shows the time-delay for SE and SEP calculations. At SE level, the first resonance appears above 4 eV and a second one appears as a bump centred at around 12.5 eV. At SEP level, we can clearly identify two broader peaks: one at 2.65 eV that corresponds to the well known π^* resonance, and another one at 6.14 eV. The second resonance has not been identified before and it does not have a corresponding feature in the SE cross section. For this reason, we assigned it mixed shape core-excited character (the resonance is also visible in both elastic and inelastic cross sections calculated at CC level; see later).

Due to the presence of a large number of pseudoresonances above 8 eV, it is not possible to identify in the time-delay a feature that would correspond to the SE resonance found at 12.5 eV: other SEP calculations (see Table III) place this resonance around 9-10 eV. Given the $\sim$2 eV shift of the π^* when polarization is included in the modelling (i.e. when going from the SE to the SEP calculation), we would expect this resonance to appear around or below 10.5 eV in the SEP time-delay. The cross section, see Figure 3 shows a very wide peak

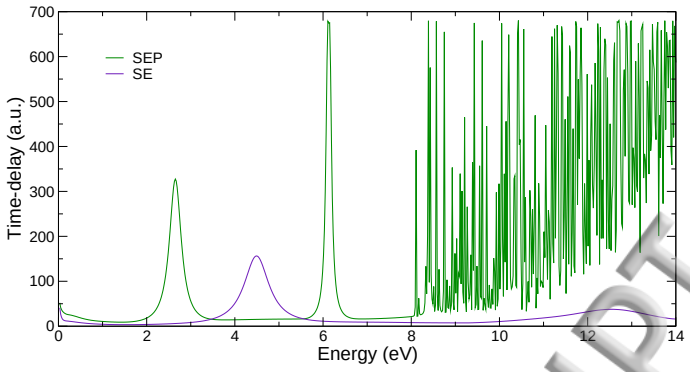

FIG. 2. Time-delay as a function of electron energy. The green line correspond to our SEP calculation using 35 VOs and the purple line correspond to the SE calculation using 10 VOs. All other parameter are the same in the two calculations.

centred around 10.4 eV that might be resonant in nature. The eigenphase sum (not shown) shows an increase of approximately 2π in the energy range 7-13 eV, although the structure associated to the pseudoresonances makes it difficult to ascertain this with confidence. There is therefore some indication that one or two wide resonances could be present in the 7-13 eV energy range.

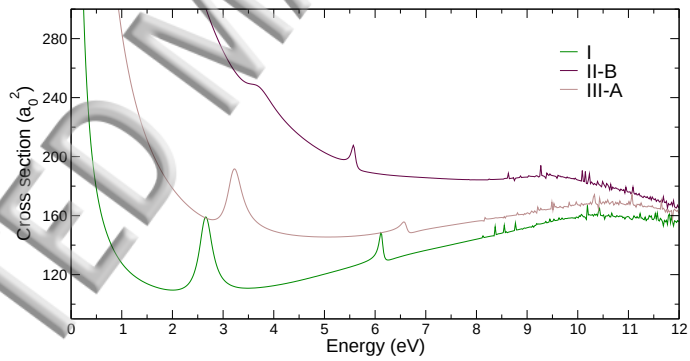

FIG. 3. Elastic cross section calculated at SEP level for the three conformers of alanine indicated in the figure. No Born-based correction to account for higher partial waves has been included.

As already stated, the 6.14 eV resonance is not present in earlier calculations. In particular, it does not appear for this conformer in the earlier R-matrix calculations of Fujimoto *et al.* although two other conformers did show the presence of a wide resonance around 8 eV. Those calculations used a more compact basis set, and consequently a smaller R-matrix radius. In order understand the difference between ours and those R-matrix calculations, we performed two tests. First, we run a calculation using the parameters (basis set, number

TABLE II. Resonance positions (in eV) for alanine conformers ('Conf.') I, II-B and III-A calculated at SEP level: the time-delay analysis was used to locate the fist two resonances while the position of the third resonance was estimated from the cross section. The values marked with an F were obtained by us using the parameters of Fujimoto's *et al.*. The dipole moment (in Debye), μ, of the conformers determined in the R-matrix calculations is listed in the last column.

Conf.		1^2A	2^2A	3^2A	μ
I	Ours	2.65	6.14	≈10.4	1.49
		2.75^F	-	$\approx 9.5^F$	1.42^F
	Fujimoto *et al.*	2.59	-	≈9.70	1.35
II-B	Ours	3.64	5.58	≈9.43	5.1
	Fujimoto *et al.*	3.14	8.03	≈9.77	6.15
III-A	Ours	3.24	6.58	≈10.5	1.8
	Fujimoto *et al.*	2.59	-	≈9.32	1.77

of VOs, R-matrix radius, etc.) of Fujimoto *et al.*: we confirmed no resonance is present between the π^* and the broad 9-10 eV one. Then, we run SEP calculations for two other conformers investigated by Fujimoto *et al.* (the geometries of these are from Császár[24]): one, conformer II-B, for which Fujimoto located a 2 eV wide resonance at 8.16 eV and another, conformer III-A, for which no intermediate resonance was found. Our calculations describe a resonance of 0.1-0.2 eV width in the energy range 5.5-6.5 eV for all three conformers, visible in the cross section (see Figure 3). Given the consistent presence of this resonance for the three conformers it seems unlikely to be an artefact of our improved calculation. As we will see later, the resonance can be correlated to DEA products. Also present in conformers II-B and II-A is a very wide feature centred in the energy range 9.5-10.5 eV that is consistent with that found in conformer I and that could indicate the presence of one or two shape resonances. The results for the three conformers are summarized in Table II.

At CC level, we identify in the time-delay three resonant features at 3.16, 6.50 and 10.45 eV, (these resonances are clearly visible in the elastic cross section in Figure 5) that correspond to the resonances discussed so far. Table III summarizes the pure shape resonances found in our calculations and the data available in the literature. The SEP position and width of the first resonance are both in agreement with other calculated values. The

CC calculation places the π^* resonance at higher energies, probably due to an incomplete description of polarization effects. The higher energy resonance is also slightly shifted to higher energies and its width is much smaller than in the literature. The mechanism of formation for this higher energy resonance is still not well-established: it has been suggested that it is associated with the σ^* unoccupied orbital of the hydroxyl group[10].

TABLE III. Position and width (in brackets) of the pure shape resonances identified in our SE/SEP/CC calculations, as well as theoretical and ETS results from the literature. In the case of Panosetti *et al.*, we quote the range in which several higher energy shape resonances appear.

		1^2A	2^2A
Ours	SE	4.49 (0.64)	12.5 (3.05)
	SEP	2.65 (0.28)	10.4?
	CC	3.16 (0.36)	10.47 (0.12)
Theory	Panosetti *et al.*[4]	2.78 (0.14)	9.7-10.9
	Fujimoto *et al.*[6]	2.59 (0.35)	9.70 (2.19)
	Nunes *et al.*[7]	2.5	9.50
Exp.	Aflatooni *et al.*[3]	1.8	-

B. Core-excited resonances

Figure 4 shows the time-delay obtained in our CC calculations. The positions and widths (when possible) were obtained by fitting the resonances in this time-delay using the Breit-Wigner formula. The shape π^* resonance discussed in the previous section is clearly visible in the time-delay at 3.16 eV. Additional features can be seen at 7-7.2 eV, around 8.5 eV and then above 10 eV. The very narrow features tend to correspond to excitation thresholds, although some might correspond to Feshbach resonances which tend to lie very close to the excitation thresholds. Due to the complexity of the time-delay we have not characterized the features above 10.5 eV although we observe the clear presence of some resonances above 11 eV. To help characterize the resonances, we looked at the elastic and inelastic cross sections, presented in Figure 5. We also used the gradual inclusion of VOs to help to identify the resonances: if a peak moves when the number of VOs changes, it

Shape and core-excited resonances in alkaline

corresponds to a res ...on dependent.

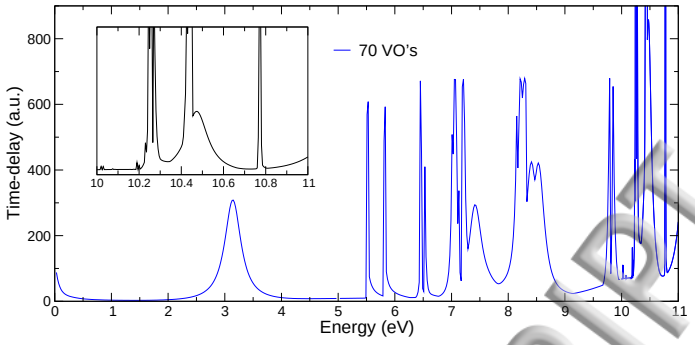

FIG. 4. Time-delay as a function of electron energy, calculated at CC level including 70 VOs. The very narrow spikes correspond to excitation thresholds. The inset shows the Lorentzian peak corresponding to the shape resonance at 10.47 eV.

Table IV summarizes all the resonances identified. We emphasize that these may not be all the electronic resonance present in this system in the 0-10.5 eV range: overlapping resonances may not have been separated and, more significantly, narrow Feshbach resonances may have been missed.

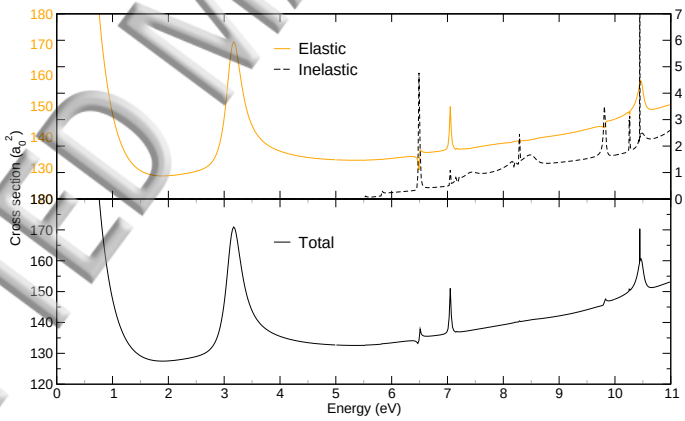

FIG. 5. Elastic, total electronically inelastic and total cross sections calculated at CC level. Upper panel: orange line, elastic cross sections; dashed black line, inelastic cross sections. Lower panel: total cross section. Note that the scale for the inelastic cross section in the upper panel is indicated on the right-hand side. No Born-based correction to account for higher partial waves has been included.

The second resonance identified by us (at 6.5 eV in the CC calculations) has not been

described by earlier theoretical work, but anion yields in DEA experiments can be linked to it (see next section). The resonance, of mixed shape core-excited character, is clearly visible in the inelastic cross section. Another resonance is present around 7.05-7.15 eV: we have been unable to fit the time-delay and provide a more accurate position or a width. The resonance is, clearly, fairly narrow and is visible in both the inelastic and elastic cross sections; it could have mixed character or be a Feshbach resonance associated to the 2^1A state at 7.197 eV in our calculations.

Three resonances are present in the 8-9 eV energy range, the higher two overlap significantly. These resonances are visible in the inelastic cross section but not the elastic one. We believe these are core-excited shape resonances and we cannot provide a width for them. Another resonance visible in the inelastic cross section (and also, though less clearly, in the elastic one) is present at 9.82 eV. No target excited states are present in this energy range in our calculations, so the resonance is probably be associated to one of the states around 8.2-8.3 eV and it's a core-excited shape resonance.

Finally, a broad resonance is present at 10.47 eV: structure is observed both in the elastic and inelastic cross sections. This corresponds to a pure shape resonance. A very narrow spike is visible in both the inelastic and total cross sections around the same energy: this seems to be a threshold effect, rather than a resonance. Earlier calculations have only identified shape resonances. In addition to the π^* resonance at low energies, Fujimoto *et al.* and Nunes *et al.* identified a shape resonance around 9.5-9.7 eV. Panosetti *et al.*[4] identified two (overlapping) resonances around 9.9 eV and a further one at 10.91 eV. Our 10.45 eV shape resonance could correspond to some of these resonances, although the widths are very different. Alternatively, the mixed character resonance at 9.82 eV could correspond to at least one of those seen by Panosetti *et al.* at about the same energy; in this case, the 10.47 eV resonance would correspond to that identified by them at 10.91 eV.

C. Link to DEA results

Ptasińska *et al.*[8] identified 9 anions in their DEA spectrum, the most abundant of which was the dehydrogenated alanine. They linked all the observed DEA peaks to three resonances: the well known π^* shape resonance, and two core-excited resonances around 5.5 and 9 eV they hypothesise are associated to the first and second excited states of alanine.

TABLE IV. Resonance positions and widths (in brackets, below the corresponding resonance position, when available), in eV, for all resonances identified in our calculations. "Ch" indicates the character: "S", shape; "M", mixed shape-core-excited; "CE", core-excited; "F" Feshbach. Also listed are the theoretical results from Panosetti *et al.*[4], Fujimoto *et al.*[6] and Nunes *et al.*[7] and the experimental results of (a) Aflatooni *et al.*[3], (b) Ptasińska *et al.*[8], (c) Vasil'ev *et al.*[9] and (d) Scheer *et al.*.[10] For the DEA results, we have followed Ptasińska *et al.* and grouped those peaks for different anion yields that are sufficiently close to potentially correspond to a single resonance. The vertical dots indicate that that the experimental resonance above could also correspond to our calculated resonances in that row.

	This work			Theory	Experiments
No.	SEP	CC	Ch.		
?					$1.27^{b,d}$ 1.2^{c}
1^2A	2.65	3.16	S	2.78^{4} 2.59^{6} 2.5^{7}	1.8^{a}
	(0.28)	(0.355)		(0.14) (0.35) —	
2^2A	6.14	6.50	M		5.5^{b} 5.60^{d} $\sim 6^{c}$
	(0.11)	(0.07)			
3^2A	-	7.05-7.15	M/F?		⋮
		(<0.1)			
4^2A	-	7.41	CE		7.63^{d}
		(0.27)			
5^2A	-	8.18	CE		⋮
6^2A	-	8.42	CE		⋮
7^2A	-	8.53	CE		⋮
8^2A	-	9.82	M	9.89^{4} 9.90^{4}	9.0^{b} 8.5-9^{c}
		(0.09)		(1.48) (0.94)	
9^2A	10.4?	10.47	S	9.5^{7}	⋮
		(0.12)	–	9.70^{6} 10.91^{4}	
				(2.19) (1.94)	

The first peak in their signal for the dehydrogenated alanine anion is at 1.27 eV, the same position found by Scheer *et al.*.[10] whereas Vasil'ev *et al.*[9] locates the peak at 1.2 eV.

This is around 0.5 eV below the position of the π^* determined in Aflatooni *et al.*'s ETS experiments and below all calculated positions for this resonance. Therefore, DEA at this energy seems unlikely to correspond to a direct attachment to this resonance. A more likely explanation is given by Abouaf[11]: H detachment (from OH) at this low energies probably occurs via direct electron attachment to the tail of an extremely wide σ^* resonance located at higher energies. We are unable to detect evidence of this resonance in our calculations, but is well known that these extremely wide resonances are hard to model and identify. The second peak in this DEA signal, at 1.42 eV, is assigned to H detachment from the C atom. Again, we think it is unlikely this peak comes from direct attachment to the π^* resonance and suggest it may again be due to another resonance or to a different conformer present in the experiment. The ion yield fragment with mass to charge ratio of 72 (corresponding to the anion produced by abstraction of OH or NH_3) has a peak centred around 1.7 eV. This value is much closer to the position of the π^* resonance as determined by ETS experiments and calculations. Panosetti *et al.* point out that, in their calculations, the π^* resonance shows a nodal plane across the COH bond.

The DEA experiments of Vasil'ev *et al.* and Ptasińska *et al.* show peaks in some anion yields at energies between 2.3 and 3.2 eV. The only resonance energetically close in our calculations is the π^* resonance.

The peaks in the H^- signal in the results of Ptasińska *et al.* are located at 5.7 and 9.0 eV. All other anions produced also display peaks in their signal at similar energies (except the dehydrogenated alanine for which there is no peak around 9 eV). Taking into account the fact that our resonances appear at higher energies due to an incomplete description of polarization effects, there are two resonances that could lead to DEA in the 5-6 eV range: one located at 6.5 eV (6.14 eV in our SEP calculations) and the other one at 7.05-7.15 eV. Both these resonances are relatively narrow (widths of 0.07 and <0.1 eV respectively). In the case of the anion production in the 8.8 to 9.6 eV energy range, we think it is either related to the pure shape resonance we locate at 10.45 eV in our CC calculations (but are unable to identify in the SEP calculations) or to the mixed character resonance we locate at 9.8 eV.

V. CONCLUSIONS

R-matrix calculations have been performed for electron collisions with alanine at the SE, SEP and CC levels of approximation. This has enable us to provide the first computational description of the core-excited resonances of this molecule.

The known pure shape π^* resonance is well described at every level of approximation and in good agreement with the earlier calculations. ETS experiments locate it at least 0.7 eV below. Agreement between different calculations and methods is poorer for the second shape resonance located at 9-10 eV.

Seven core-excited resonances have been identified but, due to the lack of symmetry of alanine, it has only been possible to determine the widths of some of them. Use of the software TIMEDELn[32] could help improve the fit of the time-delays and provide a better description of these resonances. No attempt has been made to identify the parent states of the resonances. Among these is a mixed character resonance that we observe in our SEP calculations around 6-6.5 eV that has not been reported by others. We propose a link between DEA anion yields and some of our resonances.

We believe the resonance spectrum of alanine produced in this work is likely to be incomplete: overlapping resonances and Feshbach resonances may have been missed and those appearing in our calculations above 10.5 eV have not been characterized. Further studies are required to provide a consistent and accurate description of the resonant spectrum of this aminoacid.

VI. ACKNOWLEDGEMENTS

This work used the ARCHER UK National Supercomputing Service (http://www.archer.ac.uk). It was supported by Fundação para a Ciência e a Tecnologia (FCT-MCTES), Radiation Biology and Biophysics Doctoral Training Programme (RaBBiT, PD/00193/2012); UID/Multi/04378/2013 (UCIBIO); UID/FIS/00068/2013 (CEFITEC); and scholarship grant number SFRH/BD/106031/2015 to A Loupas.

REFERENCES

[1] J. D. Gorfinkiel and S. Ptasińska, J. Phys. B **50**, 182001 (2017).

[2] I. Bald, R. Čurík, J. Kopyra, and M. Tarana, in *Nanoscale Insights into Ion-Beam Cancer Therapy*, edited by A. V. Solov'yov (Springer International Publishing, Cham, 2017) pp. 159–207.

[3] K. Aflatooni, B. Hitt, G. A. Gallup, and P. D. Burrow, J. Chem. Phys. **115**, 6489 (2001).

[4] C. Panosetti, I. Baccarelli, F. Sebastianelli, and F. A. Gianturco, Eur. Phys. J. D **60**, 21 (2010).

[5] M. Fujimoto, J. Tennyson, and S. E. Michelin, Eur. Phys. J. D **68**, 300 (2014).

[6] M. Fujimoto, E. V. R. Lima, and J. Tennyson, J. Phys. B: At. Mol. Opt. Phys. **49**, 215201 (2016).

[7] F. B. Nunes, M. H. F. Bettega, and S. d'Almeida Sanchez, J. Chem. Phys. **145**, 214313 (2016).

[8] S. Ptasińska, S. Denifl, P. Candori, S. Matejcik, P. Scheier, and T. D. Märk, Chem. Phys. Lett. **403**, 107 (2005).

[9] Y.V.Vasil'ev, B.J.Figard, V.G.Voinov, D.F.Barofsky, and M.L.Deinzer, J. Am. Chem. Soc. **128**, 5506 (2006).

[10] A. M. Scheer, P. Mozejko, G. A. Gallup, and P. D. Burrow, J. Chem. Phys. **126**, 174301 (2007).

[11] R. Abouaf, Chem. Phys. Lett. **451**, 25 (2008).

[12] B.P.Marinkovič, F.Blanco, D.Šević, V.Pejčeva, G.García, D.M.Filiponić, D.Pavlovič, and N.J.Mason, Int. J. Mass Spec. **277**, 300 (2008).

[13] J. Tennyson, Physical Reports **491**, 29 (2010).

[14] "https://gitlab.com/uk-amor/ukrmol/ukrmol-in," (2019).

[15] Z. Mašín *et al.*, Computer Phys. Comm. (in preparation).

[16] J. M. Carr, P. G. Galiatsatos, J. D. Gorfinkiel, A. G. Harvey, M. A. Lysaght, D. Madden, Z. Mašín, M. Plummer, J. Tennyson, and H. N. Varambhia, The European Physical Journal D **66**, 58 (2012).

[17] Z. Mašín and J. D. Gorfinkiel, The Journal of Chemical Physics **135**, 144308 (2011).

[18] P. G. Burke, *R-Matrix Theory of Atomic Collisions: Application to Atomic, Molecular and Optical Processes* (Springer, 2011).

[19]A. U. Hazi, Physical Reviews A **19**, 920 (1979).

[20]F. T. Smith, Physical Reviews **118**, 349 (1960).

[21]R. D. Johnson III Editor, "NIST Standard Reference Database Number 101," (2011).

[22]V. P. Gupta, V. D. Gupta, and C. Mehrotra, Int. J. Quant. Chem. **20**, 373 (1981).

[23]P. D. Godfrey, S. Firth, L. D. Hatherley, R. D. Brown, and A. P. Pierlot, J. Am. Chem. Soc. **115**, 9687 (1993).

[24]A. G. Császár, J. Phys. Chem. **100**, 3541 (1996).

[25]G. Bazsó, E. Najbauer, G. Magyarfalvi, and G. Tarczay, J. Phys. Chem. A **117**, 1952 (2013).

[26]H. M. Jaeger, H. F. I. Schaefer, J. Demaison, A. G. Császár, and W. D. Allen, J. Chem. Theor. Comput. **6**, 3066 (2010).

[27]A. Osted, J. Kongsted, and O. Christiansen, J. Phys. Chem. A **109**, 1430 (2005).

[28]S. Kumar, A. K. Rai, S. B. Rai, D. K. Rai, A. N. Singh, and V. B. Singh, J. Mol. Struct. **791**, 23 (2006).

[29]H.-J. Werner, P. J. Knowles, G. Knizia, F. R. Manby, M. Schütz, P. Celani, W. Györffy, D. Kats, T. Korona, R. Lindh, A. Mitrushenkov, G. Rauhut, K. R. Shamasundar, T. B. Adler, R. D. Amos, A. Bernhardsson, A. Berning, D. L. Cooper, M. J. O. Deegan, A. J. Dobbyn, F. Eckert, E. Goll, C. Hampel, A. Hesselmann, G. Hetzer, T. Hrenar, G. Jansen, C. Köppl, Y. Liu, A. W. Lloyd, R. A. Mata, A. J. May, S. J. McNicholas, W. Meyer, M. E. Mura, A. Nicklass, D. P. O'Neill, P. Palmieri, D. Peng, K. Pflüger, R. Pitzer, M. Reiher, T. Shiozaki, H. Stoll, A. J. Stone, R. Tarroni, T. Thorsteinsson, and M. Wang, "Molpro, version 2015.1, a package of ab initio programs," (2015), see http://www.molpro.net.

[30]M. Tarana and J. Tennyson, J. Phys. B: At., Mol. Opt. Phys. **41**, 205204 (2008).

[31]A. Loupas, K. Regeta, M. Allan, and J. D. Gorfinkiel, The Journal of Physical Chemistry A **122**, 1146 (2018), https://doi.org/10.1021/acs.jpca.7b11865.

[32]D. A. Little, J. Tennyson, M. Plummer, C. J. Noble, and A. G. Sunderland, Computer Physics Communications **215**, 137 (2017).

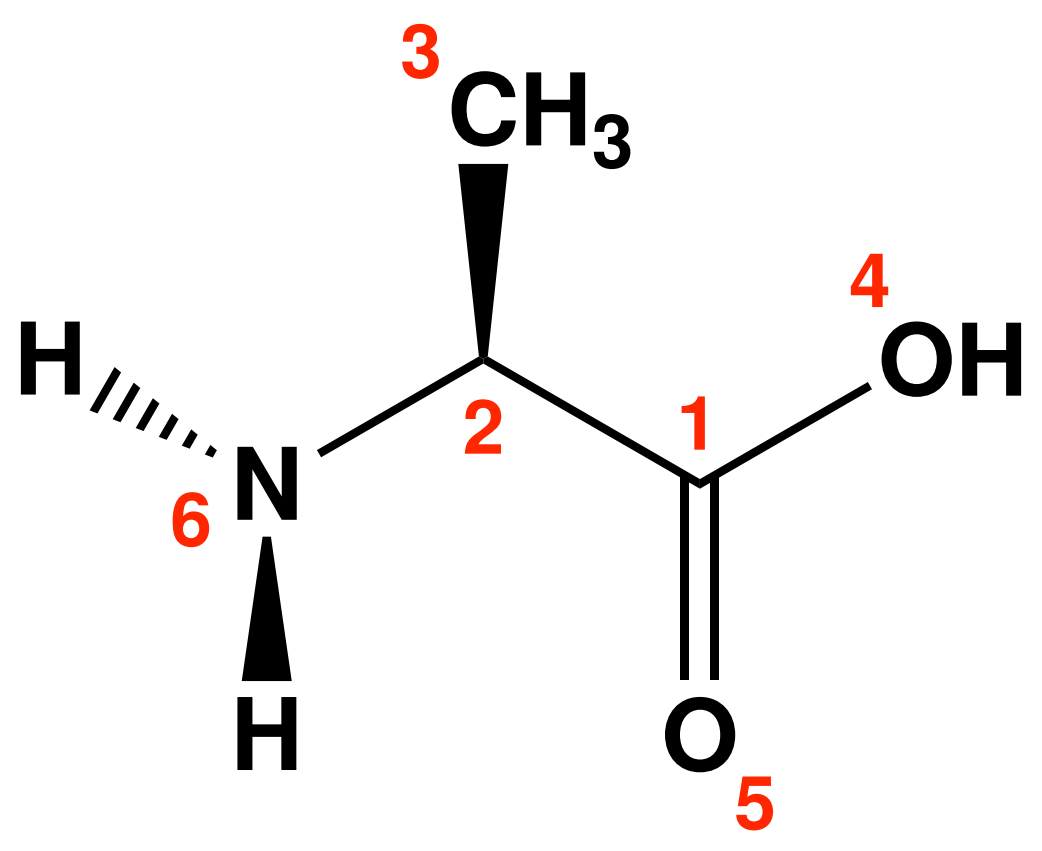
3
CH3
4
OH
H
2
1
6
N
H
O
5